International Journal on Advanced Science Engineering Information Technology

Vol.10 (2020) No. 4
ISSN: 2088-5334

Estimation the Natural Frequencies of a Cracked Shaft Based on Finite Element Modeling and Artificial Neural Network

Enass H. Flaieh[a,1], Farouk Omar Hamdoon[b], Alaa Abdulhady Jaber[a,2]

[a] *Mechanical Engineering Department, University of Technology, Baghdad, Iraq*
E-mail: [1]20057@uotechnology.edu.iq; [2]20039@uotechnology.edu.iq

[b] *College of Engineering, Wasit University, Wasit, Iraq*
E-mail: fomar@uowasit.edu.iq

***Abstract*— The early detection of faults in rotating systems considers an integral approach that has received considerable attention from the industrial sector, as it contributes to preventing catastrophic failures in machines. In this research, the natural frequencies of a shaft, when it is healthy and when cracks with different depths are introduced, have been calculated. The deviation of the computed natural frequencies from the healthy ones is counted as a sign of the presence of an abnormality in the system. For this intention, the finite element analysis (FEA) method based on ANSYS software has been utilized to obtain the first five natural frequencies of the shaft when there is a crack of different severity at different positions. The results of the FEA are used for designing an artificial neural network (ANN) model that can be easily used to predict the first five natural frequencies of the shaft based on just the crack's position and depth. Finally, the predicted natural frequencies by the deigned ANN have been compared to their peers that were computed using the FEA method. The absolute error percentage has then been calculated and used to get an indication of how close the result of both techniques is. The recorded highest error percentage was 0.67%, which is quite small and referring to that the designed ANN can accurately predict the natural frequencies of rotating systems.**

***Keywords*— rotating shaft; fault detection; finite element analysis; ANSYS; artificial neural network.**

I. INTRODUCTION

Detection of cracks in shafts represents one of the most reliable fault diagnosis methods, as it helps in preventing catastrophic failures from taking place [1, 2]. Thus, many techniques have been developed to predict the occurrence of cracks in shafts; for instance, Shen and Taylor [3] introduced a method for simple crack identification in a beam with one pair of symmetric cracks. The introduced method is proposed for an on-line and non-intrusive damage detection technique for vibrating systems. However, interesting work was conducted to detect the added ice mass on wind turbine blades [4]. The change in the blade natural frequencies due to the added mass was considered for this purpose. The blade was experimentally simulated as a cantilever beam, and the experimental modal analysis was performed on it. The extracted results were utilized for training an artificial neural network (ANN) model that is designed for estimation of how much added mass. In another paper, the researchers have studied the crack properties and effect of their variations on the natural frequencies of beams [5]. An experimental database was used to design and train an ANN to predict the crack location and depth. The input to the ANN was the natural frequencies, whereas the crack depth and location were the output of the ANN. The obtained ANN result was verified with experimental results, and high agreements between them were found. Also, Dahak, et al. [6] have investigated the effect of cracks on the natural frequencies of beams. A finite element model of Euler–Bernoulli was presented with a damaged element. Concerning the damaged element, the stiffness matrix was calculated based on the theories of fracture mechanics, as the inverse of the flexibility matrix. It was shown that the crack could be located based on the correlation between the shape of the measured frequencies with those obtained by the finite element method. The integrity of the presented method was conducted using ANSYS APDL and experimental tests. The results showed that the predicted values were close to the correct ones with an error of less than 1.5% for localization and less than 10% for the quantification.

Al-Shudeifat and Butcher [7] investigated the effect of crack depth on the vibration amplitudes of a rotor-bearing-disk system. Two crack models were presented, which are the open and breathing crack models. Two solutions were derived for both cracks type, finite element models, and general harmonic balance. The higher vibration amplitudes

at the backward whirl appear at the earlier crack depth than those at the forward whirl for both models of cracks. It was noticed that the resonance peaks at the second, third, and fourth sub-harmonic frequencies emerge as the crack depth increases. Moreover, Gounaris, et al. [8] presented a method to determine the crack depth and location for a transverse surface crack in a beam. The crack was simulated as a local compliance matrix of six degrees of freedom. To excite the beam, a harmonic force or moment with a known amplitude was employed, where the first measurements were taken in the direction of excitation. In contrast, the other measurements were obtained in the direction where the coupling effect due to occurring of crack. It was noticed that at small cracks, the direct response was minimal, while the coupled response changes substantially to detect the small cracks. Similarly, the transverse vibration of a clamped beam with transverse crack was modeled for the aim of studying the effect of crack parameters, such as the relative crack's position and depth, on the natural frequencies of the beam [9]. The modeling procedure was done using the finite element and neural network techniques. The theoretical findings were validated with experimental results, and high compatibility between them was found.

In terms of crack shape effect, Gounaris and Papadopoulos [10] developed a circular cracked element that has 12 coupled degrees of freedom for a Timoshenko shaft considering the effects of the gyroscopic moments. The proposed analysis was utilized to develop an identification technique for crack depth and location. The method was based on measuring the coupled vibrations in rotating shafts that are caused by a single excitation in bending direction while measuring in the axial direction. Also, Orhan, et al. [11] introduced a new crack model, unlike the commonly known V-shape crack. The study carried out using the free vibration analysis of an orthotropic cracked cantilever beam. The effect of crack depth on natural frequency was investigated both numerically and experimentally for both the new model and the V-shape model and compared with each other. It is concluded that the results were not sensitive to crack geometry change. The natural frequencies decrease with increasing the crack depth. The error between the finite element model and the experiments varies between 22% to 39% due to the structural instability that is caused by the higher crack length. Deokar and Wakchaure [12] presented a method for detecting an open crack type in a slender Bernoulli beam. Experimental modal analysis (EMA) on cracked and healthy beams was performed to measure the first three natural frequencies to be considered as a fundamental criterion for crack detection. 3D graphs of normalized frequency in terms of crack depth and location were plotted to locate the crack. A case study was presented to demonstrate the applicability and efficiency of the suggested method.

Generally, the presence of a crack in a rotating shaft makes it weaker and unsafe, and it may propagate to complete fracture leading to a catastrophic failure. Thus, crack detection using non-destructive techniques provides a route for avoiding catastrophic failure due to this common fault type. This study measures, using ANSYS software, the dynamic response of a full-scale shaft when different crack depths and locations are simulated to determine the shaft's natural frequencies and associated mode shapes. Then, the ANN will be used to develop an artificial system that can be able to estimate the natural shaft frequencies based on cracks information (depth and location). ANSYS outputs are going to be utilized for training the proposed ANN. However, for future work, an electronic system could be designed for automatic shaft fault detection [13].

II. Material and Method

This section discusses the performed finite element analysis (FEA) and how it can be implemented in ANSYS to analyze the considered shaft as a case study. Then, the ANN technique is presented; based on the finite element result, an appropriate ANN were designed.

A. Finite Element Modelling

In this paper, the model chosen to be analyzed is a simply supported beam of length L. ANSYS software was utilized to model a circular cross-section beam with a transverse open crack of depth a at a variable position c, as shown in Figure 1.

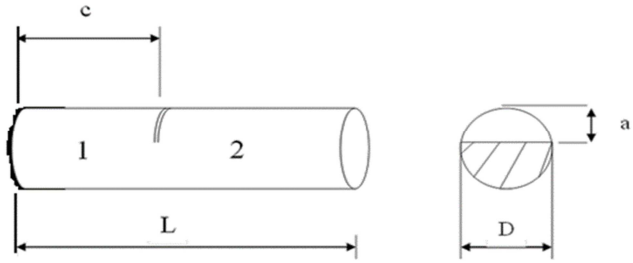

Fig. 1 Geometry of the cracked beam with crack section

The beam is divided into two parts connected by a spring (open crack). Each part is also divided into finite elements with two nodes and three degrees of freedom (DOF) at each node in the XY plane, as illustrated in Figure 2.

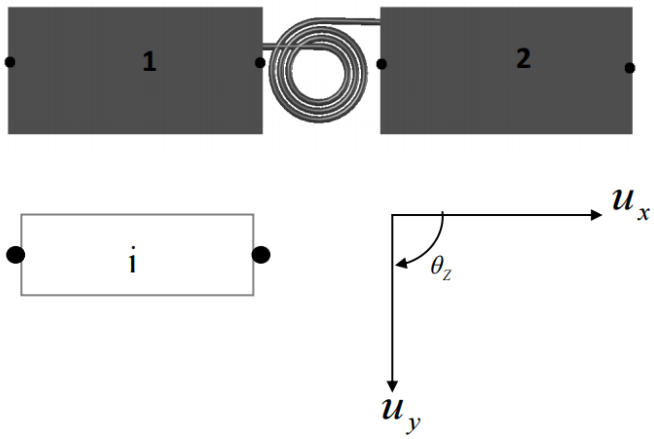

Fig. 2 The finite element model of a cracked beam

In ANSYS, the BEAM4 element is used to model these finite elements, which is a uniaxial element with six degrees of freedom at each node, which are translations and rotation in the x, y, and z directions of the nodal. The effect of the crack is modeled as a cracked massless finite element node with zero length. Equivalent flexibility coefficients have represented the crack stiffness matrix. The flexibility coefficients C_{ij} are obtained from a fracture mechanics

method that is proposed by Papadopoulos and Dimarogonas [14]. The dimensionless flexibility coefficients are calculated numerically and plotted in Figure 3. The flexibility coefficients matrix can be written according to the displacement vector (u_x, u_y, θ_z) as in [15]:

$$C = \begin{bmatrix} c_{11} & 0 & c_{13} \\ 0 & c_{22} & 0 \\ c_{31} & 0 & c_{33} \end{bmatrix}_{3x3} \quad (1)$$

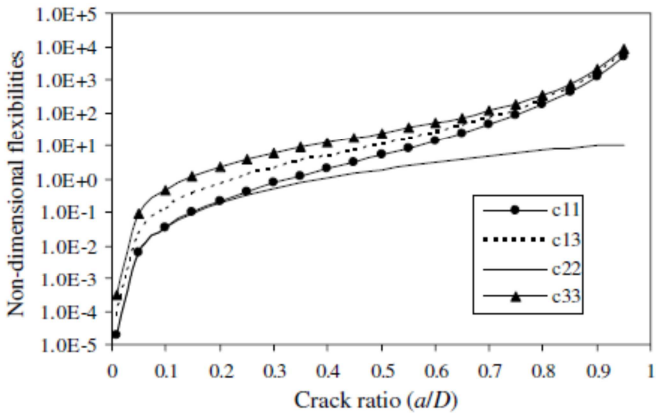

Fig. 3 Dimensionless crack flexibilities versus crack depth ratio [15]

The stiffness matrix of the nodal element is deduced based on the inverse of the above flexibility matrix (C^{-1}). Hence, the stiffness matrix of the cracked nodal element can be written as:

$$K_{CR} = \begin{bmatrix} c^{-1} & -c^{-1} \\ -c^{-1} & c^{-1} \end{bmatrix}_{6x6} \quad (2)$$

Although ANSYS is a standard tool for finite element analysis, it is similar to much other software that does not have a specific element for modeling a cracked nodal element. In ANSYS, the MATRIX27 element is available and may be utilized for modeling the cracked nodal element. The geometry of this arbitrary element is undefined, but its mechanism can be specified by stiffness, damping, or mass matrix. The matrix is presumed to be related to two nodes, and each node has six degrees of freedom, which are translations and rotation in the nodal's x, y, and z directions.

B. Artificial Neural Network

The main idea of the artificial neural networks is to produce a generalized, nonlinear mapping between input and output data sets. Generally, ANNs composed of input and output layers and at least one hidden layer. The number of hidden layers depends on how complicated the relationship is between the input and output data sets. A supervised feed-forward multilayer perceptron (MLP) (Figure 4), which is a typical type of multilayer ANNs, has been employed in this research. The input to the network is referred to as $X_1, X_2, \ldots\ldots, X_n$; the output from the hidden and output layers are referred to as O and Y, respectively. The weights matrixes that connect between the input and hidden layers and between the hidden and output layers are denoted as W_{ij} and W_{jk}, correspondingly. To calculate the output from the hidden layer and output layer, let n, l, and k represent the number of neurons in the input, hidden and output layers, thus [16]:

$$O_j = f\left[\sum_{i=1}^{n} W_{ij}\ X_i + b_j\right],\ \ j = 1, 2, \ldots\ldots, l \quad (3)$$

$$Y_k = f\left[\sum_{j=1}^{l} W_{jk}\ O_j + b_k\right],\ \ k = 1, 2, 3, 4, 5 \quad (4)$$

Where f is the activation function, b_j and b_k are the threshold values to the neurons of the hidden and output layers, respectively.

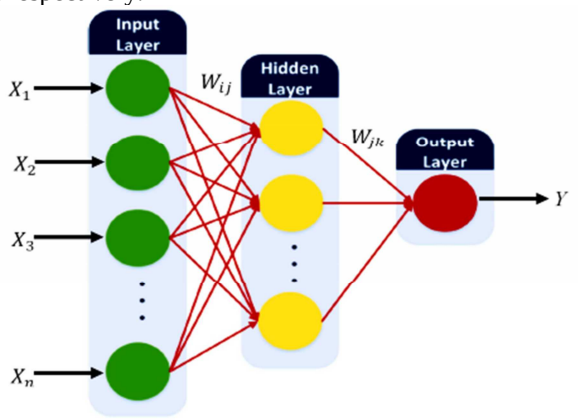

Fig. 4 Architecture of a multilayer perceptron network [16]

The designed MLP in this research is composed of three layers, which are input, hidden, and output layers, respectively. However, the neurons in the input and output layers depend on the parameters in the input data set and what is required to get from the network. Here, the network has two inputs, which are the crack position on the shaft and the crack depth ratio, and five outputs, which are the first five natural frequencies. The number of neurons in the hidden layer depends on a trial and error procedure. Moreover, the neurons contain a linear or nonlinear activation function. Commonly, a linear activation function is used in the input and output layers. In contrast, nonlinear ones are used in the hidden layers. Sigmoid activation function, which is presented in Equation 5 below, is used in the hidden layer.

$$f(x) = \frac{1}{1+e^{-x}} \quad (5)$$

To train the ANN, firstly, the input data are forwardly propagated. Then, the evaluation of the difference between the predicted (Y_k) and expected (F_k) output is conducted using Equation 6 to obtain the square error value. The error value is then backpropagated, and hence the weights between layers are got corrected based on the gradient descent method.

$$E = \frac{1}{2}\sum_{k=1}^{l}(F_k - Y_k)^2 \quad (6)$$

C. ANN Design

To design an appropriate ANN, the back-propagation training algorithm has been implemented using the neural network toolbox under the Matlab environment. To start the training process, the weights are randomly initialized. The input data (crack location and crack depth ratio) are then supplied to the input layer and consequently are passed to

the hidden layer after being multiplied with the first weight matrix (W_{ij}). In the neurons of the hidden layer, the values that come from the multiplication step are summed and passed through the sigmoid activation function to obtain the output vector of the hidden layer. This vector is then multiplied with the second weights matrix (W_{jk}) and passed to the output layer to predict the first five natural frequencies. After that, the error value is computed by comparing the predicted and target patterns. The training will be terminated if the error is within the specified limit; otherwise, the error is propagated backward to get the weights updated using as suitable training algorithm, such as the Quasi-Newton algorithm, Levenberg-Marquardt algorithm, etc. The above steps are then repeated until the error becomes within the specified limit, or the specified number of iteration is reached. After the training is appropriately completed, the network has to be tested using not previously seen data for validation purposes.

In this research, many ANN models have been tested. In each model, a different number of hidden layers with various numbers of neurons were used. Also, different training algorithms have been tried and compared based on the mean square error (MSE) value and correlation factor. However, the established best ANN contains one hidden layer with 25 neurons (Figure 5). The found best training algorithm is Levenberg-Marquardt (*trainlm*), which led to less MSE (Figure 6) with a correlation factor of 0.998.

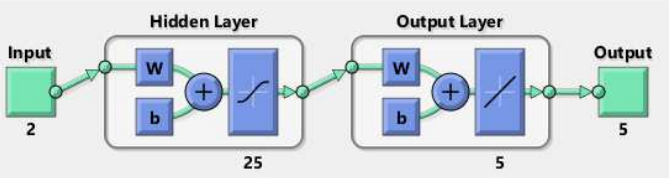

Fig. 5 The obtained best ANN design

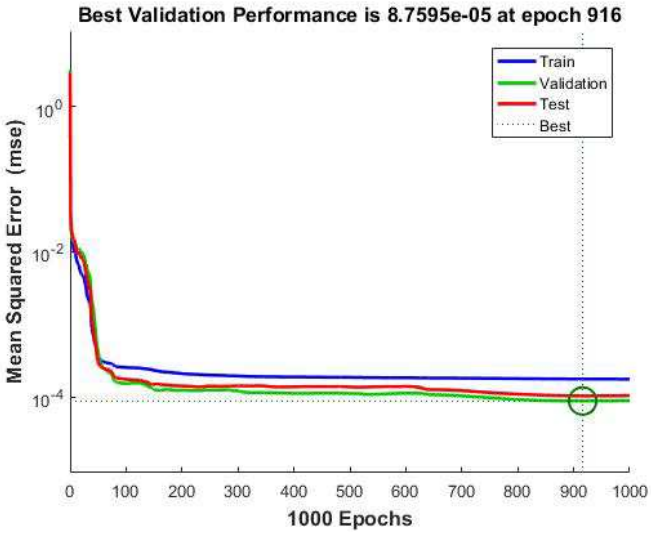

Fig. 6 The obtained best ANN design

III. Result and Discussion

The shaft has been represented as a simply supported beam having a length (L) of 500 mm, a diameter (D) of 20 mm. Its modulus of elasticity, Poisons ratio, and density are 70 Mpa, 0.3, and 2700 kg/m3, respectively. A V-shaped crack has been considered on the beam; the ratio of crack depth to shaft diameter (a/D) is varied from 0.02 to 0.5 in steps of 0.0125. This means that the maximum crack depth is 10 mm, which equals half of the shaft diameter, as in the actual situations, it is anticipated that the shaft will get broken if the crack depth becomes more than the shaft radius. The variation in the crack position relative to one of the ends was from 50 mm to 450 mm in steps of 50 mm. The purpose of varying the position and depth of the crack is to study the dynamic behavior of the shaft under different crack configurations. However, the existence of crack on the shaft leads to change its stiffness. The main assumptions here are the crack is always fully opened, and the shaft is stationary. The first five natural frequencies of the healthy and cracked (faulty) rotor that are related to each crack to depth ratio were obtained.

The variation of the first five natural frequencies is presented in Figure 7 on which the natural frequencies of the healthy shaft (ω_h) are indicated. It can be noticed that in Figure 7a, the first natural frequency starts decreasing as the crack get far from the fixed end, and it reaches its minimum value at the center of the shaft. However, it starts increasing beyond the center of the shaft until it reaches its maximum value at the other end. For the second to the fifth modes in Figure 7b to Figure 7e, it can be seen that an alternative variation in the natural frequencies as they are decreased to their minimum values and then increased back to their maximum value. This leads to producing sinusoidal curves that are denoted as the natural frequency curves [17]; these sinusoids are double, triple, quadruple, and quintuple for the second, third, fourth, and fifth modes, respectively.

In all the figures mentioned above can be inferred that almost always the healthy natural frequencies do not get affected when the crack depth ratio is 0.02 and for all the considered different crack positions. Also, a slight change/decrease in the natural frequencies can be noticed when the crack depth ratio is in the range between 0.1 and 0.25. These findings are identical with what was found by Hamidi, et al. [18], who was mentioned that the rate of change in the natural frequencies could be detectable only when the crack depth ratio gets more significant than 0.3. However, in Figure 7, the changes in the natural frequencies become apparent when the crack depth ratios are higher than 0.25 that can be related due to reduce the shaft stiffness and thus its natural frequencies as more material is removed from it when the crack depth gets increased [19].

To validate the designed ANN, a dataset that has not previously been used in designing the ANN is utilized. This dataset contains the first five natural frequencies of the shaft for the different crack to depth ratios (a/D) at various positions (P) on the shaft. The obtained validation results are shown in Table I, where P and a/D are presented in the first row and the first column of Table I, respectively. The obtained natural frequencies from the ANN are compared with their peers that were found from FEA using ANSYS software. The absolute error percentage (AEP), which is calculated using Equation 7 [20], is used to get an indication of the difference between the results.'

$$AEP = \frac{|FEA\ result - ANN\ result|}{FEA\ result} \quad (7)$$

However, the most considerable error percentages at different P and a/D are highlighted in the table for each crack position. However, the highest AEP value that can be noticed is equal to 0.67 when the crack at $P = 0.15$ and $a/D = 0.4$ at the second natural frequency. Generally, it can be inferred that all the error percentages for the different crack configurations are less than 1%, which is an excellent indication that the ANN can predict the natural frequencies of the shaft correctly.

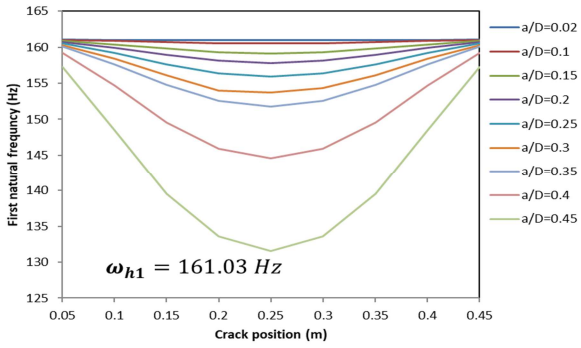

(a)

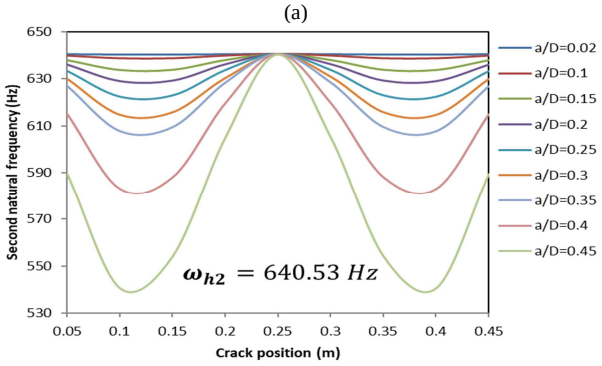

(b)

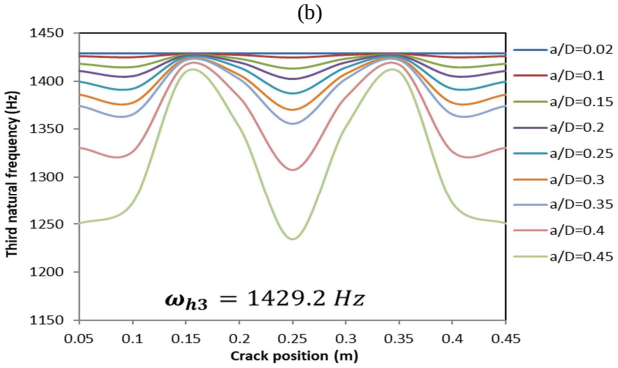

(c)

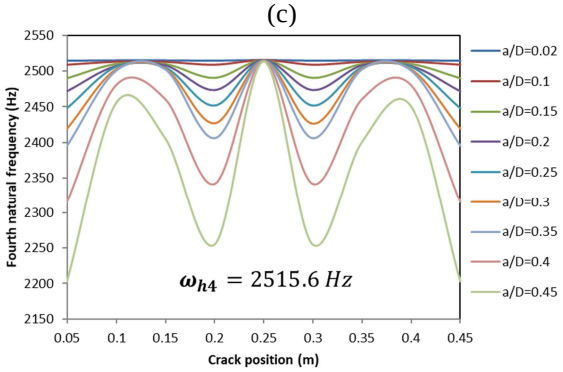

(d)

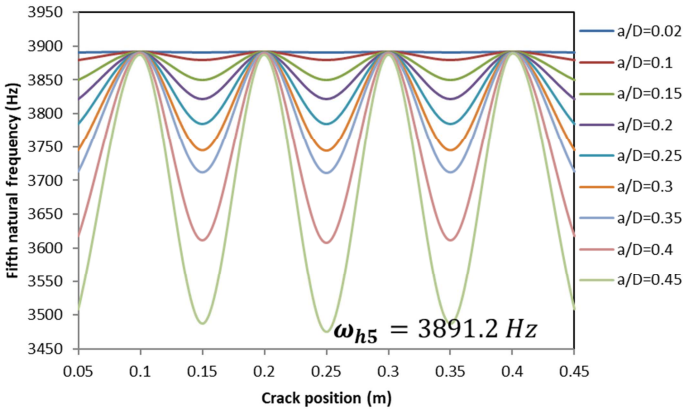

(e)

Fig. 7 The obtained first five natural frequencies based on FEA using ANSYS software

IV. Conclusion

In this paper, the possibility of using the change in the natural frequencies of a rotating system in the detection of abnormal health state was investigated. An intelligent model based on the feed-forward back-propagation artificial neural network (ANN) was designed. For this purpose, finite element analysis (FEA) was considered for modeling a stationary rotating shaft, and ANSYS software was utilized for conducting the FEA. The length and diameter of the modeled shaft are 500 mm and 20 mm, respectively. On the shaft, various crack severities at different positions were simulated, and the shaft five fundamental frequencies were obtained. It was observed that the shaft's natural frequencies are decreased, in comparison to the frequencies of the healthy shaft, as the crack depth is increased.

The FEA results were employed for training and then testing the ANN. The neural network toolbox based on Matlab 2016 was employed for ANN design. The designed ANN is composed of three layers, input, hidden, and output, with two and five neurons in the input and output layers and 25 neurons in the hidden layer. The inputs to the ANN model are the crack position and ratio of crack depth to the shaft diameter. The ANN outputs are the first five natural frequencies of the system. To validate the ANN results, a comparison with the finite element results was performed, and the absolute error percentage was calculated. The deviation between the neural network and finite element results was not significant, indicating that the designed ANN can confidently be used for predicting the natural frequencies of rotating systems.

TABLE I
PREDICATED AND COMPUTED NATURAL FREQUENCIES BASED ON ANN AND FEA

P / a/D	0.05			0.15			0.25			0.35		
	FEA	ANN	AEP %	FEA	ANN	AEP %	FEA	ANN	AEP %	FEA	ANN	Error percentage %
First natural frequency												
0.1	160.98	160.95	0.018	160.7	160.6	0.062	160.52	160.32	0.124	160.7	160.6	0.062
0.2	160.71	160.85	0.087	158.9	159.14	0.151	157.82	157.75	0.044	158.9	158.98	0.05
0.3	160.28	159.99	**0.180**	156.1	156	0.064	153.71	154.23	0.338	156.1	156.11	0.006
0.4	159.2	158.94	0.163	149.59	148.63	**0.641**	144.61	145.14	**0.366**	149.59	148.97	**0.414**
Second natural frequency												
0.1	639.83	640.14	0.048	638.72	639.6	0.137	640.52	641.20	0.106	638.72	638.23	0.076
0.2	636.03	635.63	0.062	629.33	628.83	0.079	640.51	641.14	0.098	629.33	629.65	0.05
0.3	629.92	630.65	0.115	615.66	616.19	0.086	640.49	639.54	**0.148**	615.66	617.31	0.268
0.4	614.93	613.64	**0.209**	588.06	584	**0.69**	640.46	639.82	0.099	588.06	586	**0.35**
Third natural frequency												
0.1	1426.3	1425.4	0.063	1428.7	1426.7	**0.139**	1424.8	1423.16	0.115	1428.7	1429.17	0.032
0.2	1410.6	1411.72	0.079	1426.5	1428.19	0.118	1402.1	1401.17	0.066	1426.5	1427.24	0.051
0.3	1386.1	1388.86	0.199	1423.3	1422	0.091	1369.9	1373.84	0.287	1423.3	1421.56	**0.122**
0.4	1330.3	1324.04	**0.47**	1417.2	1417.37	0.011	1307.2	1312.75	**0.424**	1417.2	1416.85	0.024
Fourth natural frequency												
0.1	2508.7	2505.86	0.113	2512.9	2511.55	0.053	2515.5	2517.31	0.072	2512.9	2509.54	0.133
0.2	2472.3	2473.4	0.044	2499	2501.41	0.096	2515.3	2515.83	0.021	2499	2501.62	0.104
0.3	2419.3	2421.12	0.075	2478.4	2476.69	0.068	2515.1	2514.48	0.024	2478.4	2480.52	0.085
0.4	2315.5	2308.76	**0.291**	2436.7	2431.4	**0.2175**	2514.6	2512.4	**0.087**	2436.7	2431.43	**0.216**
Fifth natural frequency												
0.1	3879.6	3876.1	0.09	3879.6	3882.78	0.082	3879.6	3876.76	0.073	3879.6	3879.65	0.001
0.2	3821.5	3824.07	0.067	3821.6	3817.42	0.109	3821.6	3816.75	0.126	3821.6	3822	0.0104
0.3	3744.7	3744.09	0.016	3744.3	3749.17	0.13	3743.7	3750.04	0.169	3744.3	3750.81	0.173
0.4	3618.4	3615	**0.093**	3612.1	3601	**0.307**	3608.3	3626.90	**0.515**	3612.1	3603.4	**0.2408**

REFERENCES

[1] D. Giardino, M. Matta, and S. Spanò, "A feature extractor IC for Acoustic Emission non-destructive testing," *International Journal on Advanced Science, Engineering and Information Technology,* vol. 9, pp. 538-543, 2019.

[2] G. C. Cardarilli, L. Di Nunzio, R. Fazzolari, D. Giardino, M. Matta, M. Re, *et al.*, "Acoustic Emissions Detection and Ranging of Cracks in Metal Tanks Using Deep Learning," in *Lecture Notes in Electrical Engineering* vol. 627, ed, 2020, pp. 325-331.

[3] M. H. H. Shen and J. E. Taylor, "An identification problem for vibrating cracked beams," *Journal of Sound and Vibration,* vol. 150, pp. 457-484, 1991/11/08/ 1991.

[4] S. Gantasala, J.-C. Luneno, and J.-O. Aidanpää, "Investigating How an Artificial Neural Network Model Can Be Used to Detect Added Mass on a Non-Rotating Beam Using Its Natural Frequencies: A Possible Application for Wind Turbine Blade Ice Detection," *Energies,* vol. 10, p. 184, 2017.

[5] M. S. Mhaske and S. N. Shelke, "Detection of Depth and Location of Crack in a Beam by Vibration Measurement and its Comparative Validation in ANN and GA," *International Journal of Engineering Research,* 2015.

[6] M. Dahak, N. Touat, and T. Benkedjouh, "Crack Detection through the Change in the Normalized Frequency Shape," *Vibration,* vol. 1, pp. 56-68, 2018.

[7] M. A. Al-Shudeifat and E. Butcher, "Identification of the Critical Crack Depths and Locations of Rotordynamic Systems in Backward Whirl," presented at the 7th International Workshop on Structural Health Monitoring: From System Integration to Autonomous Systems, IWSHM, 2009.

[8] G. D. Gounaris, C. A. Papadopoulos, and A. D. Dimarogonas, "Crack identification in beams by coupled response measurements," *Computers & Structures,* vol. 58, pp. 299-305, 1996/01/17/ 1996.

[9] Y. ALKASSAR, "Modal Analysis and Neural Network for Fault Diagnosis in Cracked Clamped Beam," *Romanian Journal of Acoustics and Vibration,* vol. 13, 2016.

[10] G. D. Gounaris and C. A. Papadopoulos, "Crack identification in rotating shafts by coupled response measurements," *Engineering Fracture Mechanics,* vol. 69, pp. 339-352, 2002/02/01/ 2002.

[11] S. Orhan, M. Lüy, M. H. Dirikolu, and G. Zorlu, "The Effect of Crack Geometry on the Nondestruc- tive Fault Detection in a Composite Beam," *International Journal of Acoustics and Vibration,* vol. 21, 2016.

[12] A. V. Deokar and V. D. Wakchaure, "Experimental Investigation of Crack Detection in Cantilever Beam Using Natural Frequency as Basic Criterion," presented at the International Conference on Current Trends in Technology (NUiCONE), 2011.

[13] S. Spanò, G. C. Cardarilli, L. Di Nunzio, R. Fazzolari, D. Giardino, M. Matta, *et al.*, "An efficient hardware implementation of reinforcement learning: The q-learning algorithm," *IEEE Access,* vol. 7, pp. 186340-186351, 2019.

[14] W. M. Ostachowicz and M. Krawczuk, "Coupled torsional and bending vibrations of a rotor with an open crack," *Archive of Applied Mechanics,* vol. 62, pp. 191-201, 1992/01/01 1992.

[15] M. Kisa and M. Arif Gurel, "Modal analysis of multi-cracked beams with circular cross section," *Engineering Fracture Mechanics,* vol. 73, pp. 963-977, 2006/05/01/ 2006.

[16] S. Seyedzadeh, F. P. Rahimian, I. Glesk, and M. Roper, "Machine learning for estimation of building energy consumption and performance: a review," *Visualization in Engineering,* vol. 6, p. 5, 2018/10/02 2018.

[17] S. Zhong and S. O. Oyadiji, "Identification of cracks in beams with auxiliary mass spatial probing by stationary wavelet transform," *Journal of Vibration and Acoustics, Transactions of the ASME,* vol. 130, 2008.

[18] L. Hamidi, J. B. Piaud, and M. Massoud, "A study of cracks influence on the modal characteristics of rotors," presented at the International Conference on Vibrations in Rotating Machinery, Bath, UK, 1992.

[19] D. Satpute, P. Baviskar, P. Gandhi, M. Chavanke, and T. Aher, "Crack Detection in Cantilever Shaft Beam Using Natural Frequency," in *Materials Today: Proceedings,* 2017, pp. 1366-1374.

[20] M. R. S. Reddy, B. S. Reddy, V. N. Reddy, and S. Sreenivasulu, "Prediction of Natural Frequency of Laminated Composite Plates Using Artificial Neural Networks," *Engineering* vol. 4, 2012.